forests

Article

Remote Sensing Monitoring and Evaluation of Vegetation Changes in Hulun Buir Grassland, Inner Mongolia Autonomous Region, China

Xi Dong and Chunming Hu *

State Key Laboratory of Urban and Regional Ecology, Research Center for Eco-Environmental Sciences, Chinese Academy of Sciences, Beijing 100085, China
* Correspondence: cmhu@rcees.ac.cn

Abstract: Constantly increasing vegetation changes pose serious challenges to the sustainable use of global ecosystems. Thus, facing the increasingly serious climate and ecological environment problems and improving vegetation coverage is crucial to the sustainable development of the region. Along these lines, in this work, a monitoring model of vegetation cover change was proposed and developed by using Landsat TM (1989, 1999, and 2011) and Landsat OLI-TIRS (2021) data. More specifically, it was used to assess vegetation change. Based on this model, the vegetation change in the core area of Hulun Buir Grassland was systematically analyzed., From the acquired results, the existence of spatial differences in the vegetation coverage changes in the study area were demonstrated. The total area of vegetation coverage changes was 758.95 km^2, and the area from low vegetation coverage to high vegetation coverage was 456.41 km^2, accounting for 60.14% of the total change area. The area from high vegetation coverage to low vegetation coverage was 302.57 km^2, accounting for 39.86% of the total change area, whereas the area of the area without vegetation coverage was 1963.92 km^2, accounting for 72.13% of the study area, and the overall vegetation coverage is improving. Vegetation cover change monitoring models can also be used to reveal and describe large-scale vegetation landscape changes and obtain clear vegetation change results through easy-to-obtain data; our work suggests that in the process of pursuing regional economic development and accelerating urbanization, industrialization, and agricultural modernization, human beings should assume more responsibilities and pursue the sustainable development of the natural environment. The results of this work are of great importance to further study the potential driving mechanism of the vegetation coverage changes and provide theoretical guidance for relevant managers to formulate vegetation restoration measures.

Keywords: Hulun Buir grassland; remote sensing monitoring; vegetation cover change; change monitoring model

check for updates

Citation: Dong, X.; Hu, C. Remote Sensing Monitoring and Evaluation of Vegetation Changes in Hulun Buir Grassland, Inner Mongolia Autonomous Region, China. *Forests* **2022**, *13*, 2186. https://doi.org/10.3390/f13122186

Academic Editor: Giorgos Mallinis

Received: 26 October 2022
Accepted: 16 December 2022
Published: 19 December 2022

1. Introduction

Vegetation is considered an important part of terrestrial ecosystems and plays an important role in both the security and balance of terrestrial ecosystems [1–3]. In addition, vegetation cover change is a measure of regional ecosystem stability and ecologically sustainable development, which largely reflects the change in the ecological environment and the response of vegetation to climate change and human activities [3–5]. Therefore, it is of great significance for the local environmental protection functional departments to carry out regional scale monitoring and investigate the changes in vegetation cover to guide ecological environment protection and vegetation [6].

In recent years, various works in the literature have examined the dynamic monitoring of vegetation change, spatial distribution characteristics, and the driving factors of environmental factors at the regional scale [7–11]. Fractional vegetation coverage (FVC) is also an important evaluation index to measure environmental change at the regional scale.

Therefore, the dynamic change of vegetation coverage has been extensively explored in the literature [12–15]. In recent years, global climate change, greenhouse gas emissions, global warming, and other climate issues have attracted wide attention from the scientific community. A large number of remote sensing satellites have been launched to monitor the Earth's changes. On top of that, the FVC changes, based on the development of remote sensing technology, have been also studied [13]. Based on the different time scales, the temporal and spatial dynamics of vegetation growth in Ethiopia from 2003 to 2018 were analyzed by enhanced vegetation index (EVI). The variation coefficient and driving factors of vegetation coverage (FVC) were also explored, revealing that EVI in Ethiopia mainly presents a "double peak" pattern, while there is a large spatial and temporal difference between seasons and months [11]. The relationship between the vegetation coverage and the surface runoff and Changsha volume on the Loess Plateau with typical climatic characteristics has also been investigated. However, global climate change may lead to changes in the global growth rate of FVC. More specifically, due to the construction of global ecological restoration projects, the global vegetation coverage will be increased, and climate change may cause the risk of lower vegetation coverage [16]. This situation shows that quantifying the vegetation cover change can make better contributions in solving ecological and environmental problems at the regional and global scales. With the rapid changes in the global environment, the traditional vegetation monitoring techniques have been unable to meet the needs of the regional and global scale vegetation change monitoring research. Nevertheless, with the development of remote sensing technologies, it has become possible to comprehensively monitor regional and even global vegetation changes [7,17–21]. In the study of vegetation change, a large number of works have focused on the drivers of vegetation change to predict the response of vegetation to future climate and human activities and have investigated the impact of potential management strategies [17,22–25].

Based on the existing mature remote sensing technology, a large number of works have been carried out on vegetation changes in different countries and regions around the world and in different scenarios [6,7,9,10,25–28]. Additionally, a large number of models have been developed to quantify the vegetation index for estimating the relationship between vegetation change and driving factors, including the digital change test model [9], wetland index model [29], etc. For example, Dong et.al., 2021 based on remote sensing monitoring of wetland conditions and by using NDVI as the monitoring index for vegetation change, a vegetation succession monitoring model was proposed. The authors pointed out the vegetation changes in the wetlands in the lower reaches of the Hai La Er River in the past 30 years [9]. Hao et al., 2021 quantized coastal vegetation into three periods (early, middle, and late), and the driving mechanism of vegetation coverage in coastal wetlands in China was also analyzed. It was concluded that, on all spatial scales, natural factors are the strongest driving factors of vegetation coverage in late succession. With the reduction of the spatial scale, soil and terrain played a more important role in the middle and late periods [30]. Zhang et al., 2022 took the Inner Mongolia reach of the Yellow River Basin as the study area. Based on NDVI time series data, the extreme gradient boosting method was applied to predict the changing trend of vegetation cover in the Inner Mongolia reach of the Yellow River in the next 10 years [14]. Fang et al., 2022 proposed a new ecological hydrological model (the Budyko model coupled vegetation model). The model combined the impact of climate change and vegetation change and had simple and deterministic parameters. It was revealed that vegetation growth was mainly controlled by soil moisture, and the impact of total precipitation on the regional vegetation was explained [31]. Li et al., 2022 used the trend analysis method in combination with the random forest classifier and geographic detector based on the Google Earth Engine platform. The authors analyzed the change in vegetation coverage and its driving factors. To improve the shortcomings of most previously reported works, where the contribution of natural vegetation and artificial vegetation to the macro vegetation change is confused, it is of great importance to deeply understand that agricultural activities are increasingly conducive to the increase in vegetation cover [32]. The abovementioned methods provide ideas for the study of the vegetation change. However, a large number of works have focused on the driving factors of vegetation change, whereas less attention is paid to the spatial change at the regional scale. Since there are usually different driving factors for changes in vegetation cover at different locations, the application of the conventional methods of driving factors of vegetation cover change cannot accurately characterize the driving factors of vegetation change in the ecosystems.

China is currently facing the most serious ecological environmental degradation problem in the world. Various environmental problems, such as land desertification, soil erosion, and sandstorms caused by the reduction of vegetation cover, have become increasingly serious over a long time [15]. In view of these problems, a new monitoring model of vegetation coverage change based on remote sensing data and development platforms was proposed to evaluate the vegetation change problem at the regional scale. The main goals of this work are the following: (1) the development of a new vegetation cover change monitoring model to reduce the time scale constraints of remote sensing monitoring and to scientifically characterize the vegetation changes; (2) an analysis and exploration of the reasons for the spatial differences between the changes and no changes in vegetation coverage at the regional scale; and (3) a thorough investigation of the scientific nature and limitations of the proposed algorithm and a discussion of the application prospects of the proposed algorithm.

2. Study Area and Data

2.1. Location of the Study Area

The study area in this work is located in the hinterland of Hulun Buir grassland, Inner Mongolia Autonomous Region, China, as shown in Figure 1. The geographic coordinates are 119°30′48″–120°35′36″ E 49°5′44″–19°27′15″ N, and average altitude 1480 m. The land cover types are mainly grassland, shrubland, and farmland. The area belongs to the mid-temperate continental steppe climate, which is located in the mid-high latitude temperate semi-arid region, with an annual precipitation of about 250–350 mm that is decreasing from east to west. The annual average temperature is about 0 °C, and the frost-free period is 85 to 155 days. The general characteristics of the annual climate are the following: cold and dry in winter and hot and rainy in summer. The annual temperature and the temperature date differences are large. Spring wheat, potatoes, and a small number of vegetables can be grown.

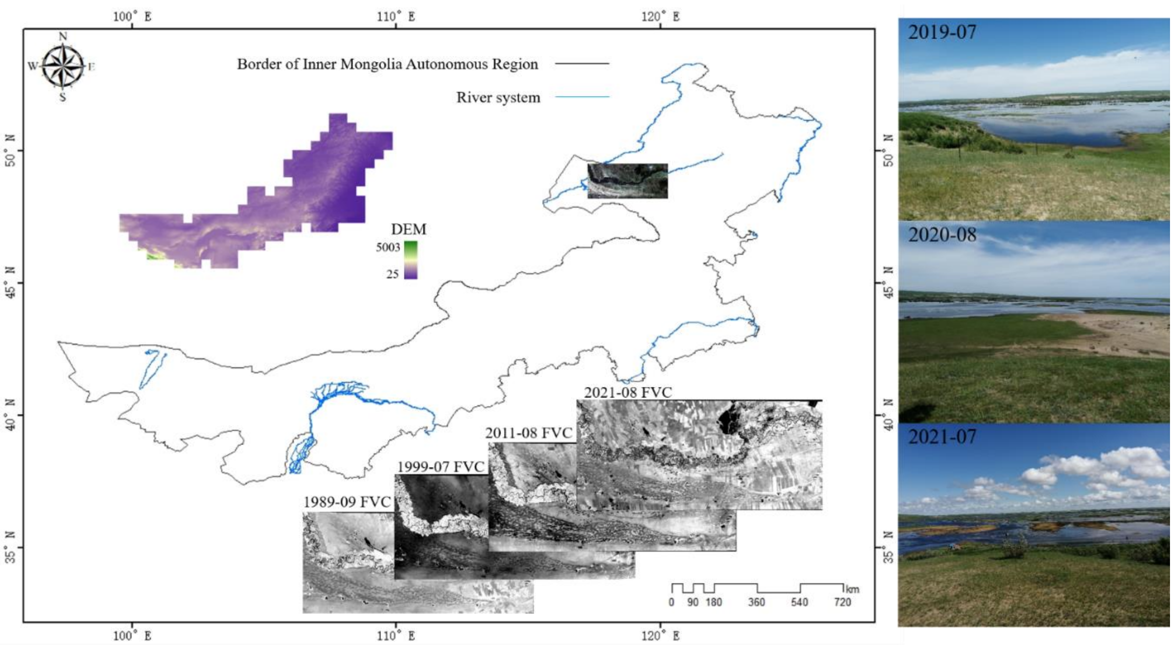

Figure 1. Study area location.

There is also an obvious desertification zone in the study area, namely Hulun Buir Sandy Land. The sandy land covers an area of nearly 10,000 square kilometers. When the former Soviet Union aided the construction of the railway, the Pinus sylvestris forests from Hulun Lake to the western suburbs of Hai La Er were completely cut down, resulting in the desertification of the land.

The study area has a wide range of lakes that vary in size but play an important role in providing habitat for water birds, maintaining biodiversity and providing valuable ecological services. Moreover, the study area has a special position in regional ecological environment protection and exhibits various ecological service functions, such as wind protection and biodiversity support.

2.2. Data Sources and Processing

Landsat satellite imagery was used to extract the vegetation coverage in the study area and to track long-term vegetation change dynamics and sand changes at the pixel level (see Sections 3.1–3.4 for details). In this work, the 1T-level image data of Landsat 5 TM and Landsat 8 OLI satellites covering the study area were obtained from the National Aeronautics and Space Administration (NASA). The data are presented in Table 1. The images cover the entire study area, and the row and column numbers are 123,026 and 124,026. The image acquisition times were on 15 September 1989, 7 August 1999, 11 August 2011, and 29 August 2021. The selected monitoring time is this period of vigorous plant growth in the region, and the data cloud cover is less than 2%. The rainfall and temperature data in the study area from 1989 to 2020 were downloaded from the China Meteorological Data Network (http://data.cma.cn, accessed on 5 June 2022).

Table 1. Landsat 5 TM/8 OLI data situation.

Satellite	Band	Nominal Spectral Location	Satellite	Band	Nominal Spectral Location
Landsat5 TM	1	Blue	Landsat8 OLI	1	Costal/Aerosol
	2	Green		2	Blue
	3	Red		3	Green
	4	Near IR		4	Red
	5	SWIR-1		5	Near IR
	6	LWIR		6	SWIR-1
	7	SWIR		7	SWIR-2
				8	Panchromatic
				9	Costal/Aerosol

The radiometric calculations were performed by using the Radiometric Calibration tool in ENVI 5.3 (Remote sensing image processing platform, the flagship product of American Exelis Visual Information Solutions.), and atmospheric corrections were made. The values of all reflectance products were between 0 and 1 [33], and the obtained reflectance products were collectively registered based on the data in August 2021. The NDVI and FVC data were calculated by the band calculation tool.

3. Research Methods

3.1. Technical Route

Figure 2 illustrates the technical flow of this work. First, the historical spatiotemporal vegetation coverage data from the four-phase Landsat images were identified, and the four-phase vegetation coverage data were classified to distinguish low, medium-low, medium-high, and high vegetation coverage areas. Then, the two periods of 1989 and 2021 were used to perform the vegetation coverage change monitoring model calculation (the operation procedure of the vegetation coverage change monitoring model is described in detail in Section 3.4), and the changing area was identified pixel by pixel between different categories. The differences in the temporal and spatial variation of the vegetation coverage in the study area were obtained. Finally, the advantages and disadvantages of the monitoring model of vegetation cover change, the spatial difference of vegetation cover change, the change process of the Hulunberg Sandy Land, and its driving factors were discussed, and the conclusions were drawn.

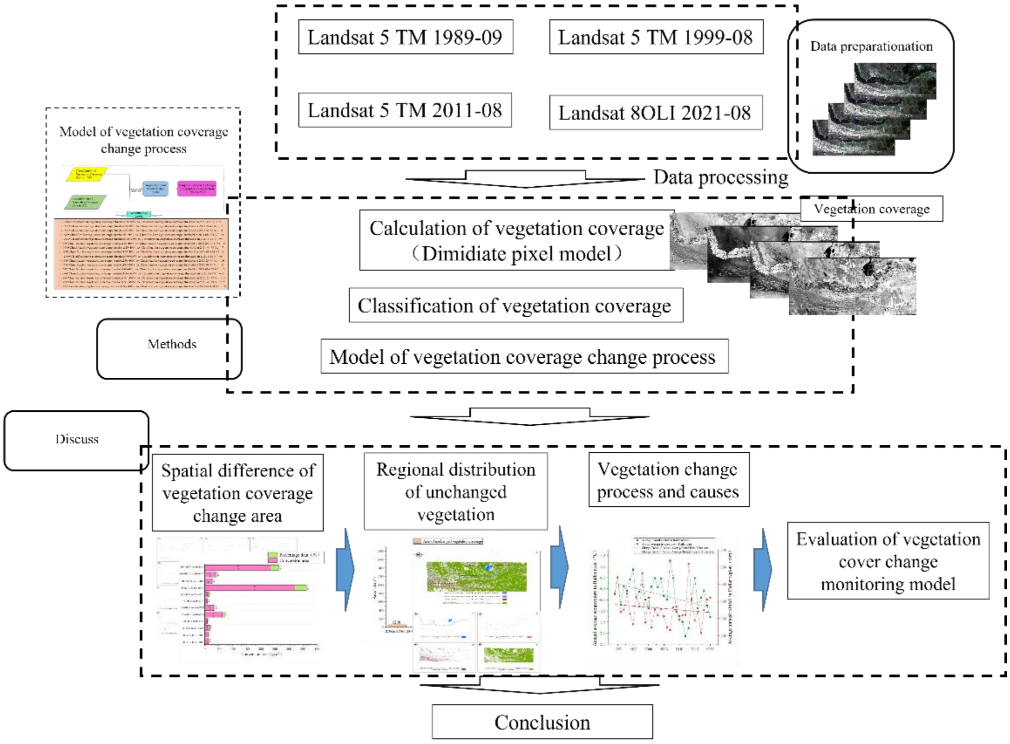

Figure 2. Research process.

3.2. *Vegetation Coverage Calculation Model*

Vegetation coverage (FVC) refers to the percentage of the vertical projected area of vegetation on the ground [34]. At present, the more practical method is to use the vegetation index (such as NDVI) and pixel dichotomy model to estimate the vegetation cover index [34]. In this work, a bipartite pixel model was used, which is a simple and commonly used linear model to characterize the historical change dynamics of the vegetation coverage [35,36]. Particularly, it was assumed that the information of a pixel is composed of vegetation and soil. As a result, the information of a pixel observed by remote sensing sensors can be regarded as the information contributed by the soil (without vegetation coverage) and the information contributed by the vegetation coverage.

The pixel binary model expresses the relationship between the remote sensing information and vegetation coverage. NDVI can well reflect the growth of vegetation in different periods and the coverage of vegetation at different locations. Therefore, on the basis of the pixel binary model, the vegetation coverage in the study area was estimated by NDVI. Its mathematical expression model is as follows [35,36]:

$$FVC = (NDVI - NDVI_{soil})/(NDVI_{veg} - NDVIs_{oil}) \quad (1)$$

Among them, $NDVI_{soil}$ is the NDVI value of the completely bare soil or no vegetation coverage area, and $NDVI_{veg}$ represents the NDVI value of the pixel completely covered by vegetation, which is the NDVI value of the pure vegetation pixel. The formula for calculating the two values is [35,36]:

$$NDVI_{soil} = (FVC_{max}*NDV_{Imin} - FVC_{min}*NDVI_{max})/(FVC_{max} - FVC_{min}) \quad (2)$$

$$NDVI_{veg} = ((1 - FVC_{min})*NDVI_{max} - (1 - FVC_{max})*NDVI_{min})/(FVC_{max} - FVC_{min}) \quad (3)$$

The key to using this model to calculate the vegetation coverage is to estimate $NDVI_{soil}$ and $NDVI_{veg}$. There are two assumptions here:

(1) When the area can be approximated, to take FVC_{max} = 100%, FVC_{min} = 0%.

Formula (1) can be changed to:

$$FVC = (NDVI - NDVI_{min})/(NDVI_{max} - NDVI_{min}) \quad (4)$$

where $NDVI_{max}$ and $NDVI_{min}$ are the maximum and minimum NDVI values in the region. Due to the inevitable existence of noise, $NDVI_{max}$ and $NDVI_{min}$ generally take the maximum and minimum values within a certain confidence range, and the confidence value is mainly determined according to the actual situation of the image.

(2) When FVC_{max} = 100% and FVC_{min} = 0% cannot be approximated in the area.

When there are measured data, the maximum and minimum values of vegetation coverage in the measured data are taken as FVC_{max} and FVC_{min}, while the NDVI of the images corresponding to these two measured data are taken as $NDVI_{max}$ and $NDVI_{min.}$

When there is no measured data, $NDVI_{max}$ and $NDVI_{min}$ are used within a certain confidence range. FVCmax and FVCmin are estimated empirically. In this work, a 95% confidence interval value for $NDVI_{max}$ and a 5% confidence interval value for $NDVI_{min}$ were chosen.

3.3. Vegetation Coverage and Classification

FVC is widely used for vegetation change monitoring in the literature, such as [22,37] and [38], whereas the value of FVC ranges from 0 to 1.

In this work, FVC was used to display the spatial distribution of vegetation in the study area. FVCs were extracted from the four-phase Landsat images, whereas the FVC values were classified using the equiclustering unsupervised classification technique. The results were then used to compare the changes in vegetation in the study area of the four-phase remote sensing images.

FVC was reclassified as "low vegetation coverage, medium-low vegetation coverage, medium-high vegetation coverage, and high vegetation coverage". In this work, the vector data of the dominant tree species in forest land in 2016 provided by Hai La Er Regional Forestry Bureau combined with three field investigations and the application of FVC classification was used to determine the FVC classification threshold low vegetation coverage, 0%–20%; medium and low vegetation coverage, 20%–40%; medium-high vegetation coverage, 40%–60%; and high vegetation coverage, 60%–100%. The critical values were included in the previous classification interval. With this classification, changes in vegetation in the study area over the past nearly three decades can be compared with changes in the current conditions.

3.4. Model of Vegetation Coverage Change Process

The vegetation coverage extracted from remote sensing images was used as a monitoring indicator to monitor vegetation changes. Through digital classification of remote sensing images at different time nodes, the vegetation cover changes were evaluated. This result demonstrates the ability of remote sensing images to monitor the time effect of vegetation changes in a long time series [9].

In our research, the classification method was used to compare the four time-varying scenarios of 1989, 1999, and 2011 based on the date of 2021 (the data obtained in this work started in 1989 since there were no images suitable for classification in the summer of 2000 and 2010; therefore, the images from the summer of 1999 and 2011 were chosen as representative). Dong et al., 2021, based on NDVI change data, proposed a vegetation change detection model for analysis and comparison of the NDVI change detection [9]. This technique easily provides a change matrix from which different transitions from vegetation cover intervals at one time to another can be visualized. After obtaining the classified images, this method can identify the changed regions as pixel-wise differences between different classes [9], which can clearly show the changed regions and the transformed classes.

On this basis, we propose a monitoring model for vegetation cover change. Figure 3 shows the operation process of vegetation cover change monitoring model. The mathematical model and operation process of vegetation cover change monitoring are as follows:

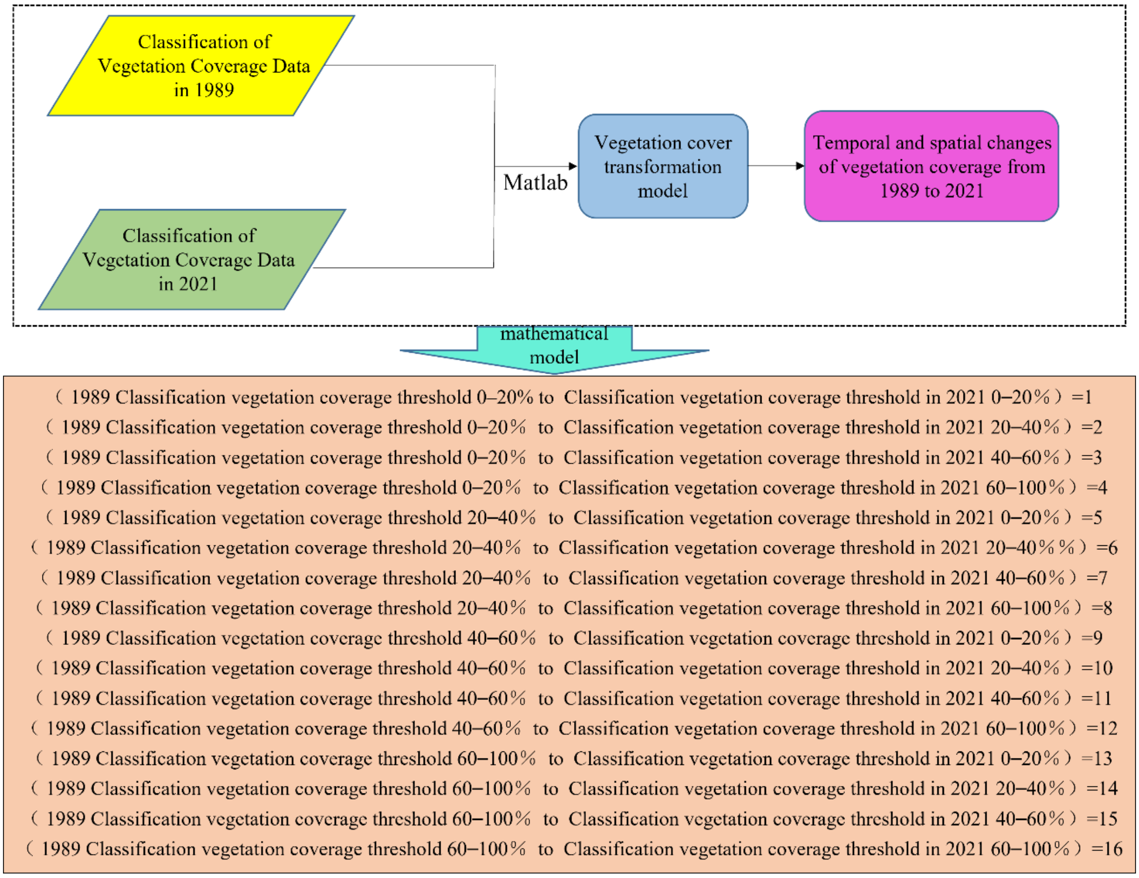

Figure 3. Vegetation cover change monitoring model operation process.

The change in the vegetation coverage is represented by a numerical value, where 1 indicates that the change in the low vegetation coverage in 1989 is the low vegetation coverage area in 2021 (i.e., no change area), and 2 indicates that the change in the low vegetation coverage in 1989 is the medium-low vegetation coverage in 2021. The value of 3 for the coverage area indicates that the low vegetation coverage in 1989 changed to the medium-high vegetation coverage area in 2021, while the value of 4 specifies that the low vegetation coverage in 1989 changed to the high vegetation coverage area in 2021. The value of 5 indicates the medium-low vegetation coverage in 1989. The change in the coverage is the low vegetation coverage area in 2021, while 6 means that the change in the medium-low vegetation coverage in 1989 is the low-medium-vegetation coverage area in 2021 (i.e., the area with no change). The change in vegetation coverage is based on this analogy.

4. Results

4.1. Vegetation Change and Spatial Distribution

This work mapped the vegetation cover in the hinterland of the Hulunbuir grassland in 1989, 1999, 2011, and 2021 to analyze the changes in vegetation over the past three decades. Figures 4–7 depict the classification of vegetation coverage in the Hulunbuir grassland hinterland during the period of vigorous summer vegetation growth at four time points in 1989, 1999, 2011, and 2021. Additionally, Figure 8 displays a column chart of the area of vegetation coverage in different classification intervals of the study area with km^2 as the unit, while the total area of the study area was 2722.87 km^2.

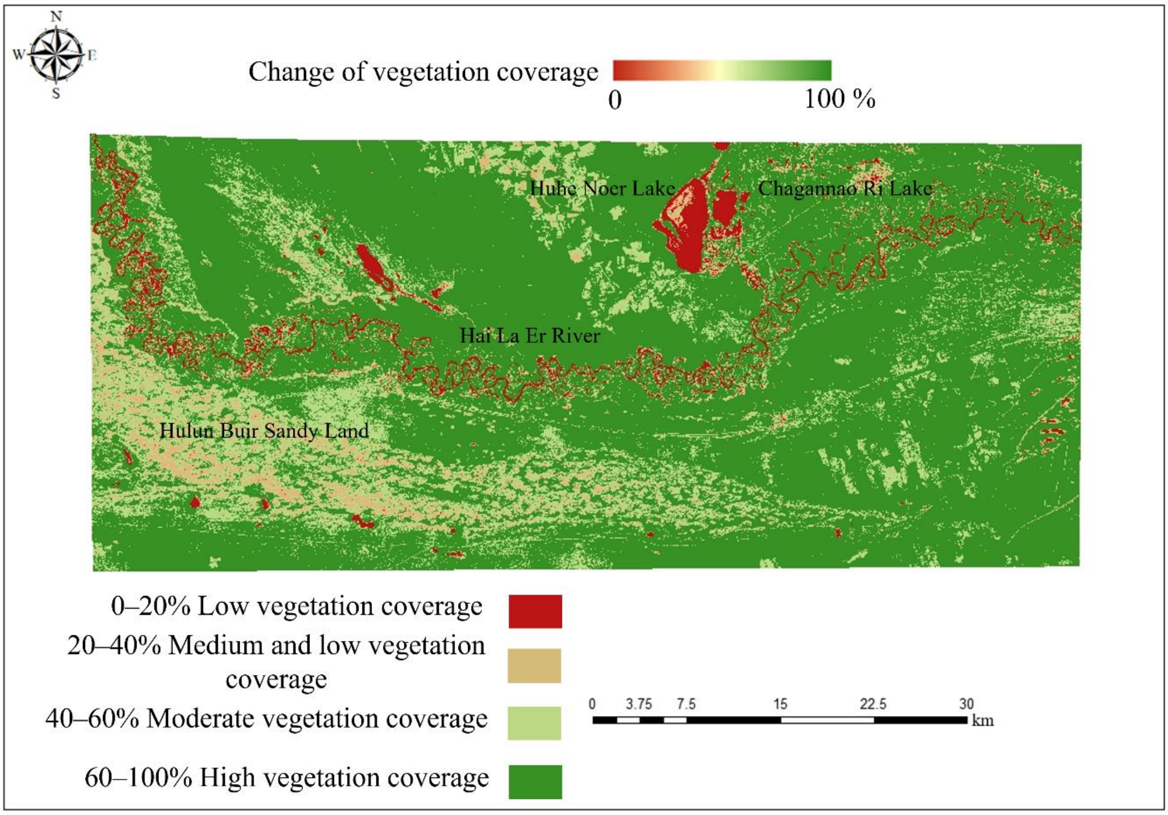

Figure 4. Vegetation coverage in the lower reaches of the Hai La Er River in 1989.

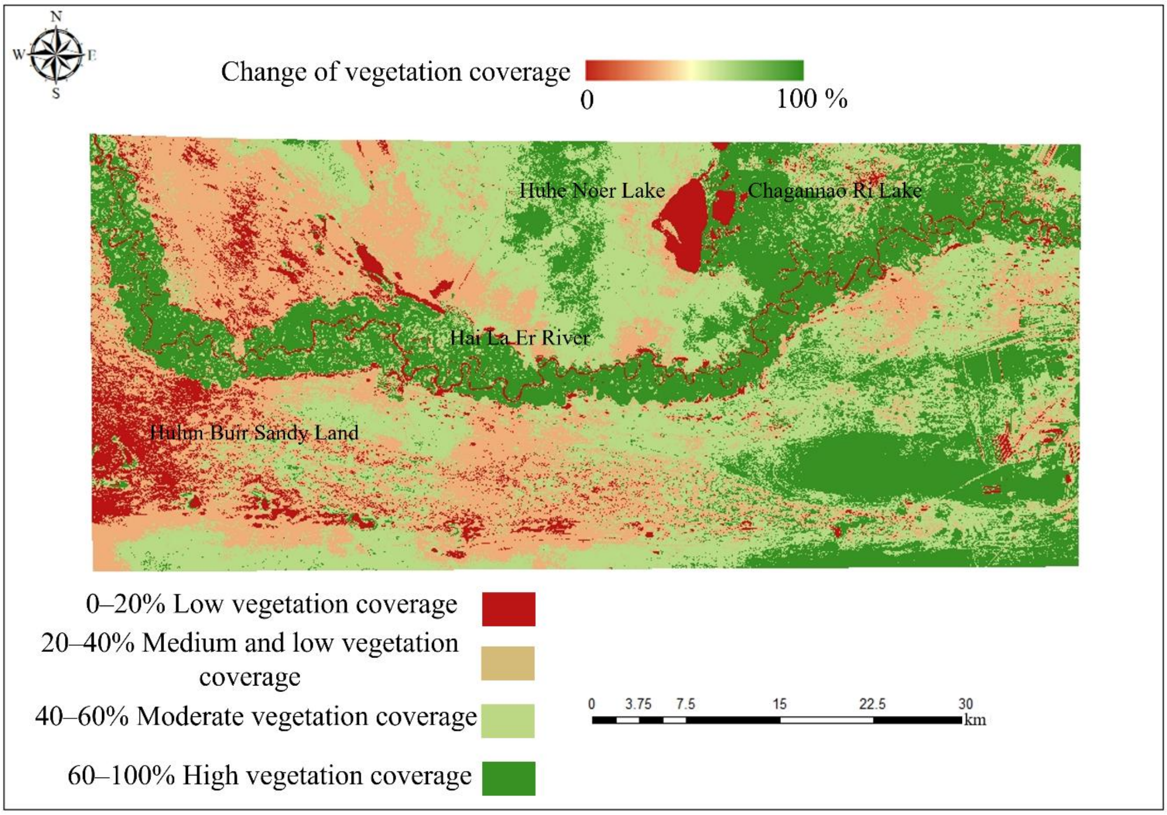

Figure 5. Vegetation coverage in the lower reaches of the Hai La Er River in 1999.

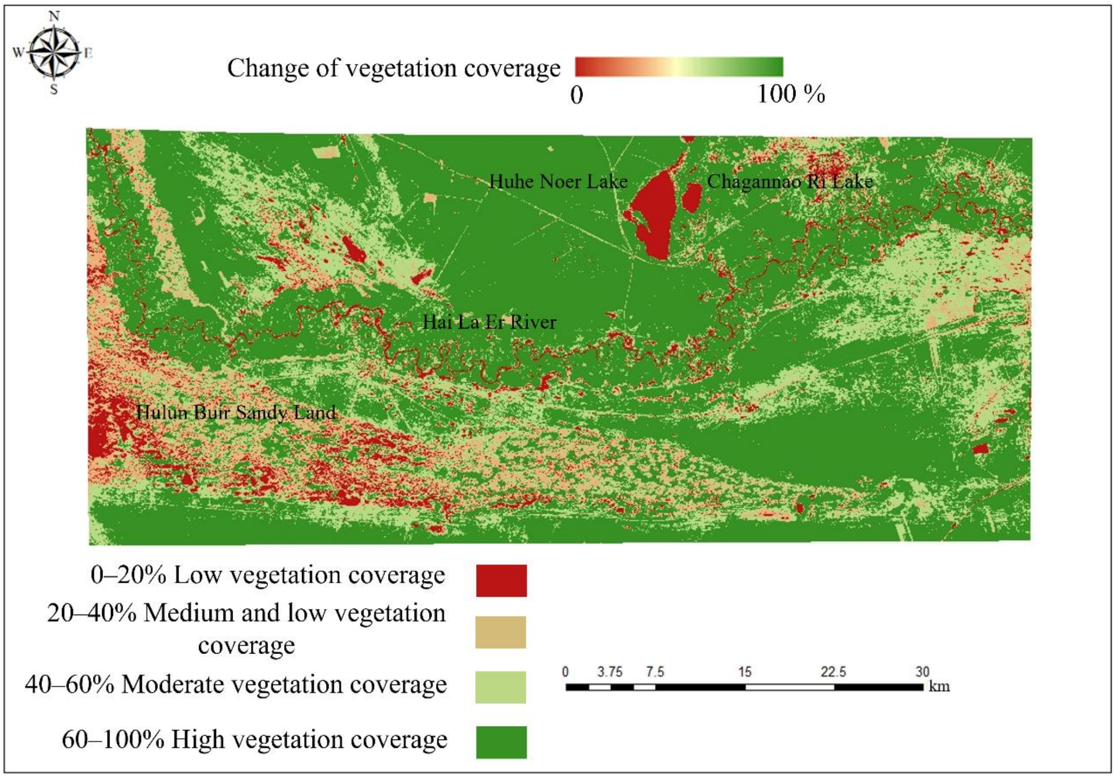

Figure 6. Vegetation coverage in the lower reaches of Hai La Er River in 2011.

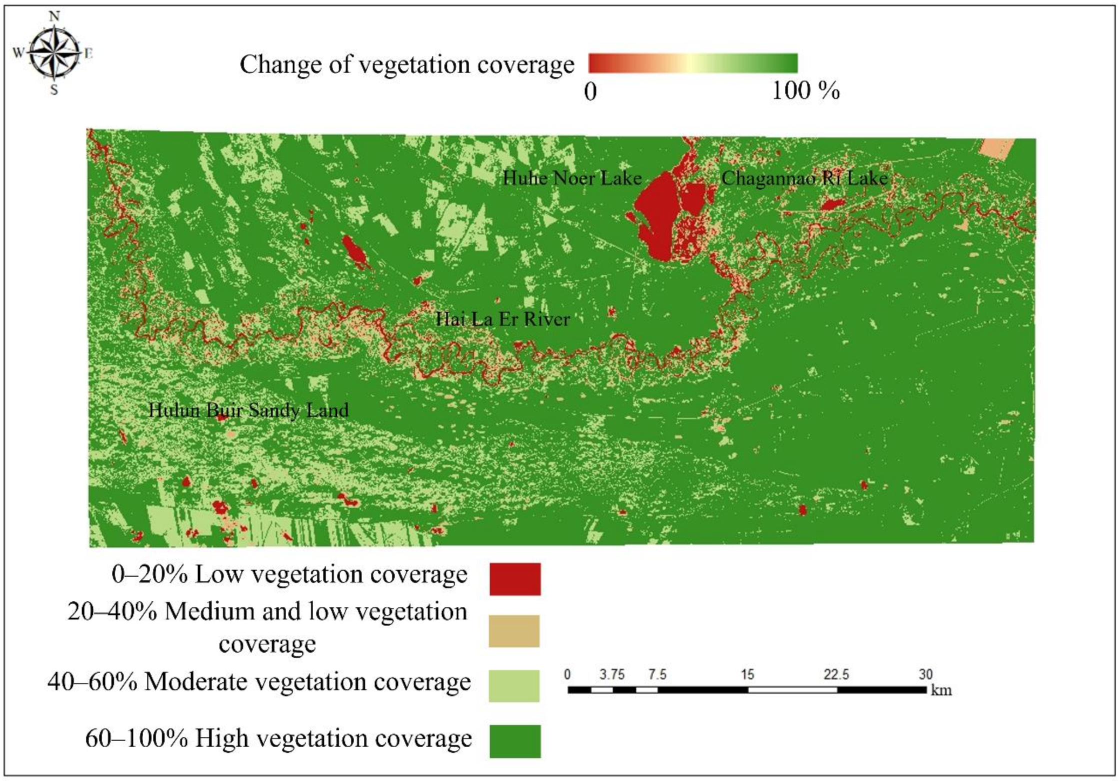

Figure 7. Vegetation coverage in the lower reaches of the Hai La Er River in 2021.

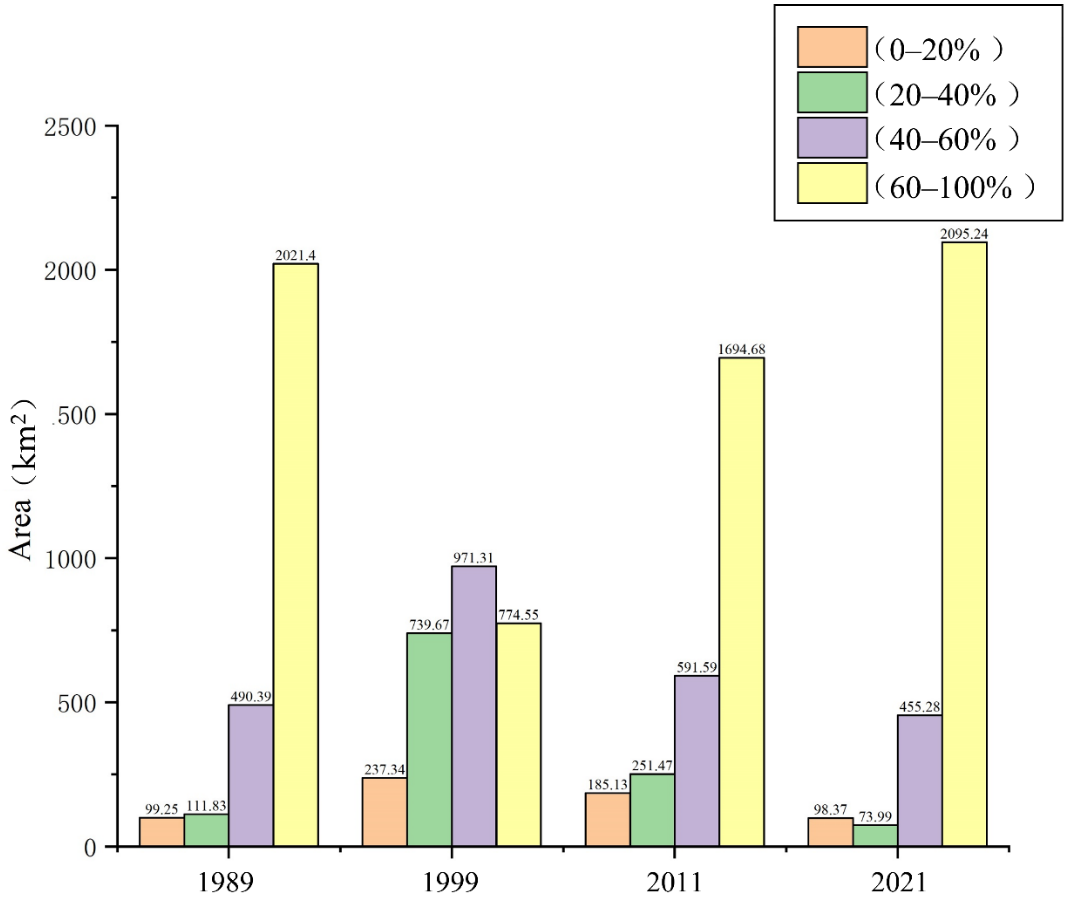

Figure 8. Areas of different vegetation coverage classification intervals in 1989, 1999, 2011, and 2021.

From 0%to 20% Low Vegetation Coverage: The 0–20% low vegetation coverage area in the study area showed a trend of first increasing and then changing. In 1989, the area of 0%–20% low vegetation coverage area was 99.25 km^2, and by 2021, its coverage area decreased to 98.37 km^2, which indicates a decrease of 0.88 km^2. At the four study time nodes, in the summer of 1999, the area covered by low vegetation coverage was the largest, at 237.34 km^2.

From 20% to 40% Moderate to Low Vegetation Coverage: The change of the medium and low vegetation coverage area can be divided into two change intervals, indicating the change situation of first increasing and decreasing and then decreasing. From 1989 to 1999, the total area of medium and low vegetation cover categories increased from 111.83 km^2 in 1989 to 739.67 km^2 in 1999, which suggests a total increase of 627.84 km^2 during this time period, an increase of 6.61 times. From 1999 to 2021, the area of medium-low vegetation coverage area decreased from 739.67 km^2 to 73.99 km^2, which indicates a total decrease of 665.68 km^2, and the change was obvious.

From 40% to 60% Medium to High Vegetation Coverage: This category displays the same change trend as the low and medium-low vegetation cover changes. More specifically, it first increased and then decreased. From 1989 to 1999, the total area of medium and high vegetation coverage categories increased from 490.39 km^2 in 1989 to 971.31 km^2 in 1999, which indicates a total decrease of 480.92 km^2 during this period. From 1999 to 2021, the area of medium and high vegetation coverage area decreased from 591.59 km^2 to 455.28 km^2, which signifies a total reduction of 136.31 km^2. From 1989 to 2021, the area of medium and high vegetation coverage area decreased by 34.59 km^2.

From 60% to 100% High Vegetation Coverage: During the study period, this category showed a clear opposite trend compared with the other three categories of interval changes. Particularly, during 1989–1999, the total area of high vegetation cover category decreased from 2021.4 km^2 in 1989 to 774.55 km^2 in 1999, which indicates a total reduction of 1246.85 km^2 during this period. From 1999 to 2021, the area of the high vegetation coverage area increased from 774.55 km^2 to 2095.24 km^2, which specifies a total increase of 1320.69 km^2. Finally, from 1989 to 2021, the area of high vegetation coverage area increased by 73.84 km^2.

4.2. Temporal and Spatial Variation of Vegetation Cover

Based on the summer data of the date 2021, vegetation cover change monitoring was conducted to examine the vegetation cover changes of the different categories of FVC in the past three decades from 1989 to 2021.

As can be observed from Figure 9, from the perspective of the spatial location of changes in the different types of vegetation coverage, the area with significant changes was located in the Hulun Buir Sandy Land, which indicates the change in the medium-high vegetation coverage in 1989 is the high vegetation coverage in 2021. At the same time, there are also areas with high vegetation coverage that have changed to medium and high vegetation coverage areas, whereas the change in location mainly occurs in the northern part of the study area. In the lower reaches of the Hai La Er River, a considerable part of the high vegetation coverage area was also degraded to the low vegetation coverage area. The areas where this change occurs are mainly located in the floodplain wetlands on both sides of the Hai La Er River.

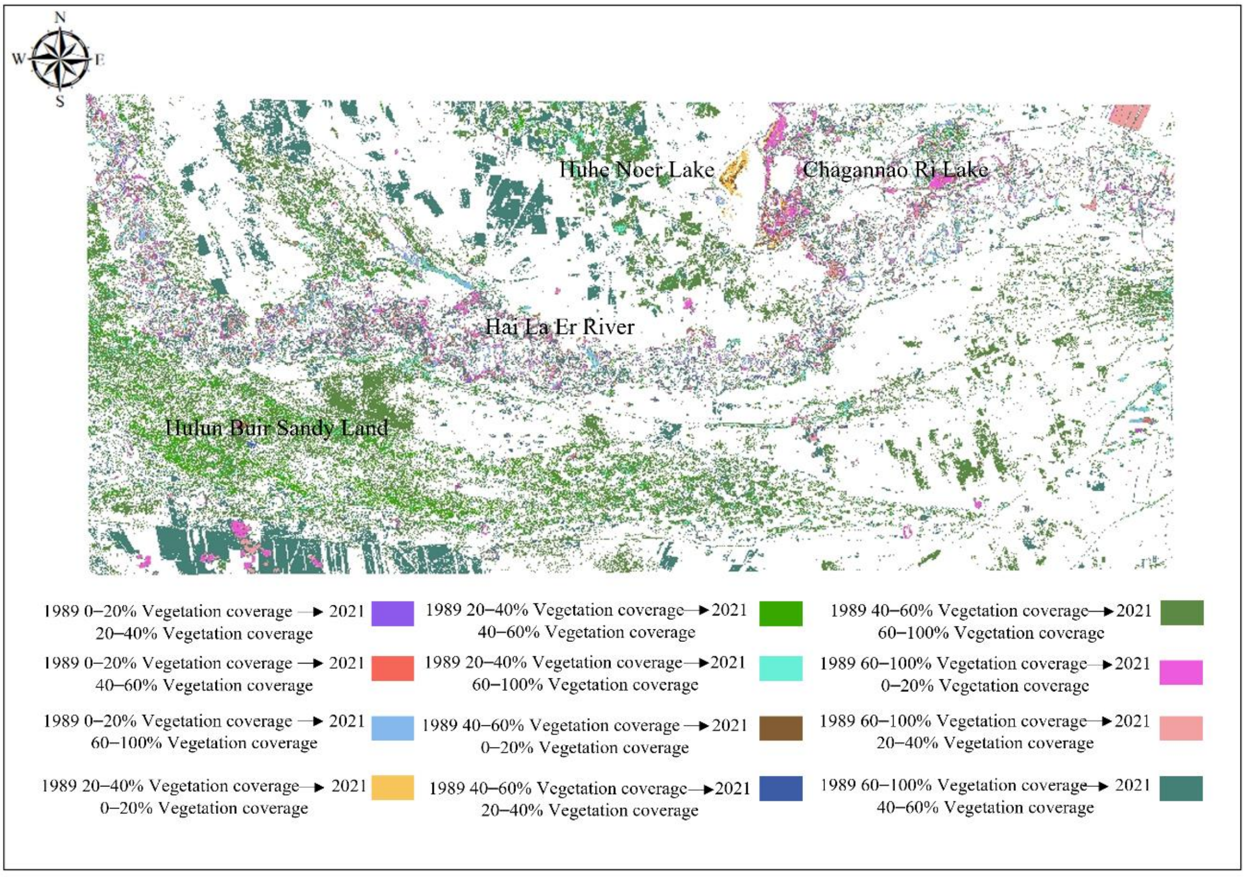

Figure 9. The succession of vegetation coverage classification intervals in the 1989–2021 time scenario.

5. Discussion

5.1. Spatial Differences in Vegetation Coverage Change Areas

Vegetation is also considered an important part of the terrestrial ecosystem and an important link to the sustainable development of the ecological environment. Undoubtedly, it plays an important role in the water cycle and the mitigation of greenhouse gas emissions in the ecosystem [1,5,16,39]. Vegetation, as an important indicator of ecosystem stability and health, has been widely explored by several works in the literature recently [4,5]. The driving force of vegetation change usually comes from human influence. For example, ecological resource protection measures, such as controlling grazing, protecting grassland, and establishing a reasonable protection mechanism can improve vegetation resistance [40].

The vegetation coverage change monitoring model developed in this work is a good example of our long-term spatial and temporal sequence of vegetation changes. Figures 10 and 11 show the changes in different vegetation coverage intervals in the past 30 years from 1989 to 2021. As can be seen, the areas with obvious vegetation coverage changes are Figure 10E,F,J,K,M. The change represented by E is that the 20%–40% medium and low vegetation coverage in 1989 changes to medium and high vegetation coverage in 2021. The main spatial area of transformation occurred in the Hulun Buir Sandy Land. The area of this transformation interval was 62.45 km^2, which accounts for 7.97% of the total transformation area. The change represented by F is the change of 20%–40% medium and low vegetation cover in 1989 to high vegetation cover in 2021. The main transformation space area that occurs is located in the west of the study area, while the area of this transformation area is 31.37 km^2, which accounts for 4.05% of the total transformation area. The change represented by J is the change from 40% to 60% medium to high vegetation cover in 1989 to high vegetation cover in 2021. The main transformation space area is located in the Hulun Buir Sandy Land study area. The area of this transformation area is 321.4 km^2, which corresponds to 41.02% of the total transformation area. It is the main vegetation transformation area in the study area for the past 30 years. The change represented by K is the change of 60%–100% medium-high vegetation cover in 1989 to low vegetation cover in 2021. The main transformation space area is located in the floodplain wetland area around Hai La Er River, Huhe Nuoer Lake, and Chagannao Ri Lake. The area of this transformation area is 23.99 km^2, which accounts for 3.06% of the total transformation area. The data results can be drawn from Figure 11. The total area of vegetation coverage changes in the study area was 758.95 km^2. The area that changed from low or above vegetation coverage to high vegetation coverage was 456.41 km^2, which accounts for 60.14% of the total change area. The area that changed from high vegetation coverage to low vegetation coverage was 302.57 km^2, which corresponds to 39.86% of the total changed area.

On the whole, from 1989 to 2021, the vegetation coverage in the hinterland of Hulun Buir grassland was improved as a whole. Since 1983, the state has implemented the policy of subscribing land to households, and herdsmen manage the pastures by themselves. Over-cultivation and over-grazing have been alleviated. These measures have had a positive impact on the protection and transformation of the Hulun Buir grassland since the 1980s [9,11]. Due to its humid climate background and with the increase in human improvement disturbance, the vegetation gradually developed from low vegetation coverage to high vegetation coverage.

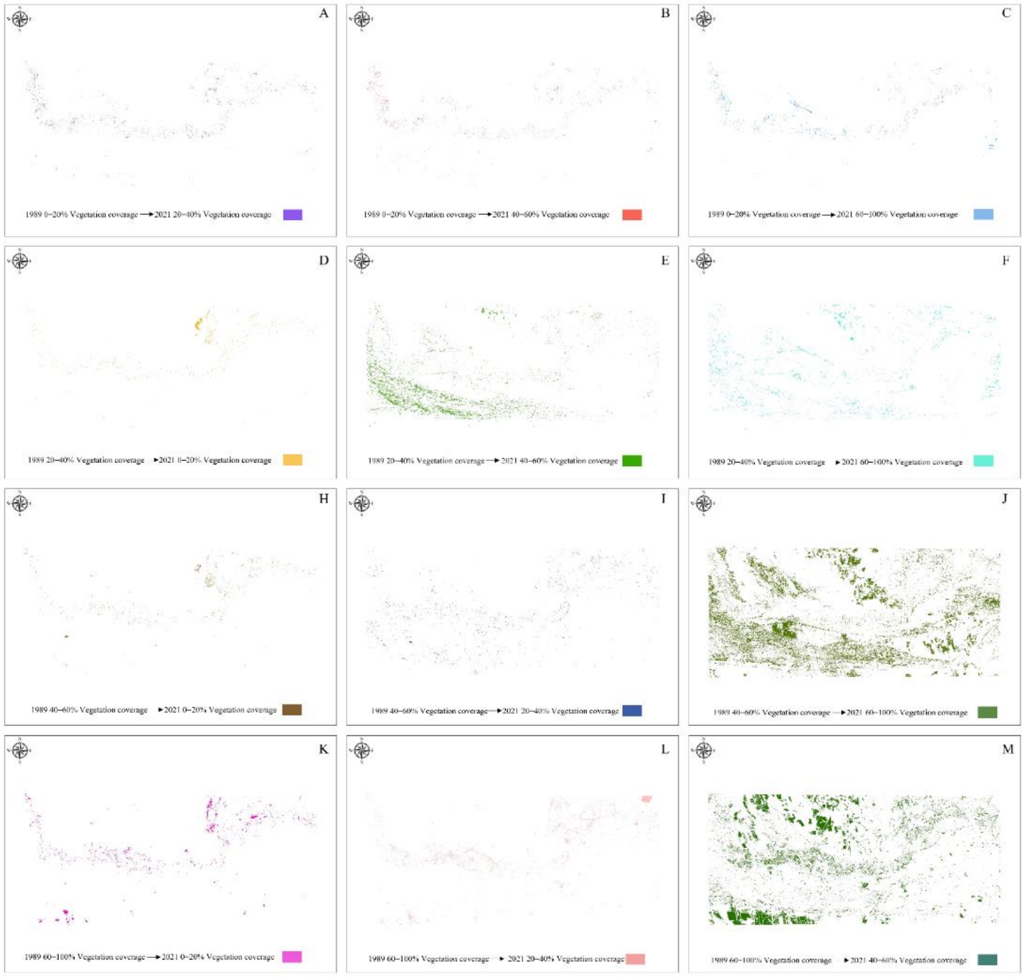

Figure 10. Changes in different vegetation coverage intervals in the past 30 years from 1989 to 2021 (**A**): the area of 1989 0–20% vegetation coverage change to 2021 20–40% vegetation coverage; (**B**): the area of 1989 0–20% vegetation coverage change to 2021 40–60% vegetation coverage; (**C**)**:** the area of 1989 0–20% vegetation coverage change to 2021 60– 100% vegetation coverage; (**D**): the area of 1989 20–40% vegetation coverage change to 2021 0– 20% vegetation coverage; (**E**): the area of 1989 20–40% vegetation coverage change to 2021 40–60% vegetation coverage; (**F**): the area of 1989 20–40% vegetation coverage change to 2021 60–100% vegetation coverage; (**H**): the area of 1989 40–60% vegetation coverage change to 2021 0–20% vegetation coverage; (**I**): the area of 1989 40–60% vegetation coverage change to 2021 20–40% vegetation coverage; (**J**): the area of 1989 40–60% vegetation coverage change to 2021 60–100% vegetation coverage; (**K**): the area of 1989 60–100% vegetation coverage change to 2021 0–20% vegetation coverage; (**L**): the area of 1989 60–100% vegetation coverage change to 2021 20–40% vegetation coverage; (**M**): the area of 1989 60–100% vegetation coverage change to 2021 40–60% vegetation coverage).

Hai La Er River is the mother river of the Hulun Buir area. In the past 30 years, the large-scale exploitation of open-pit coal mines in Hulun Buir region has led to a significant increase in industrial water consumption in the basin, resulting in unreasonable development of local water resources. At the same time, urban development and regional grazing have also an impact on the vegetation cover change of floodplain wetlands on both sides of the Hai La Er River. These negative human activities have inhibited the vegetation cover change of the Hai La Er River [9].

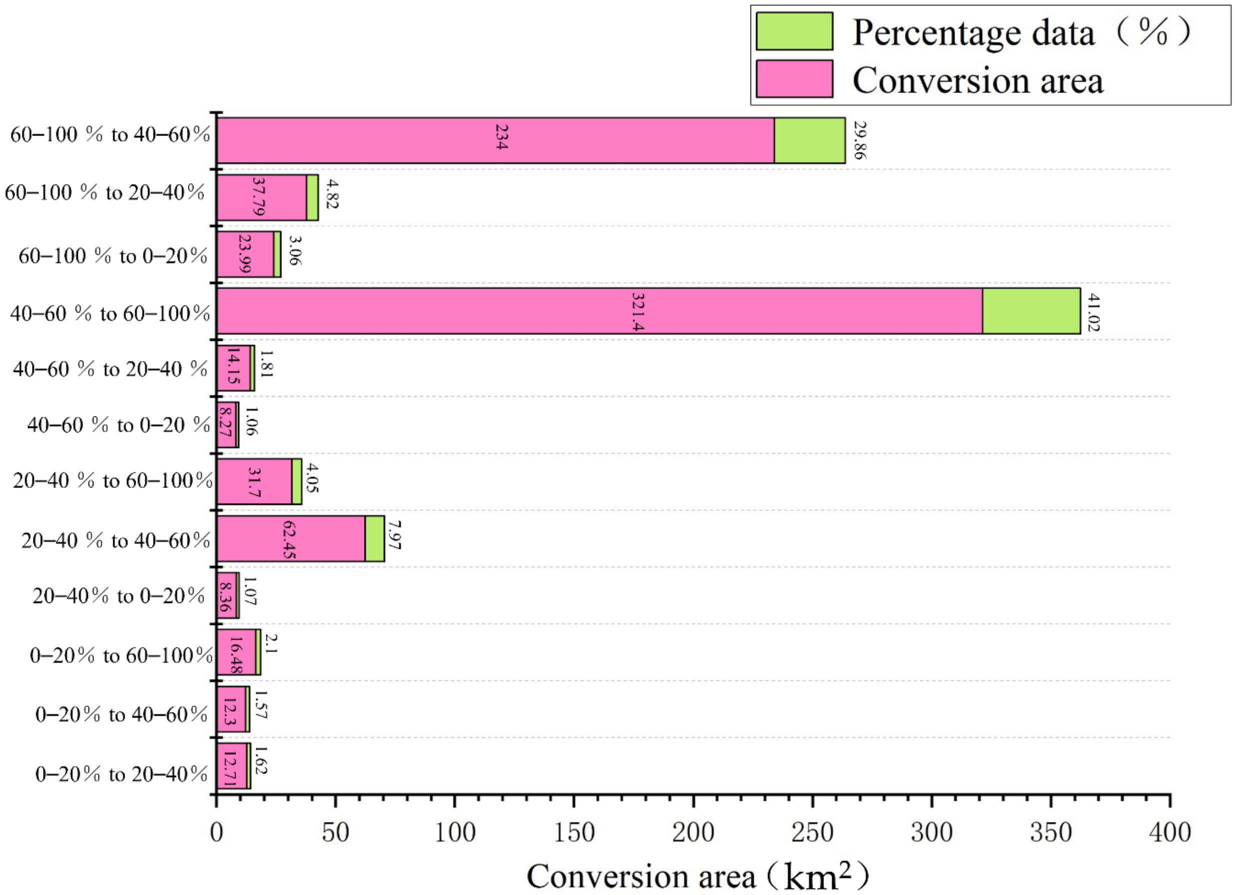

Figure 11. Successive area changes that occurred in the 1989–2021 time scenario.

5.2. Regional Distribution of No Change in Vegetation

Vegetation cover plays also an important role in terrestrial ecosystems and energy balance. Especially in areas with fragile ecological environments, the temporal and spatial changes of vegetation not only cause changes in surface parameters but also affect ecosystems and show profound interactions with the human population [11].

From a spatial point of view, the overall area of the study area without vegetation coverage in the hinterland of Hulun Buir grassland is relatively large. The total area of the study area is 2722.87 km^2, and the area without vegetation coverage is 1963.92 km^2, which accounts for 72.13% of the study area. Figure 12 depicts that the vegetation coverage in the study area has not changed. D and E show two areas with no significant changes. B represents the change from 0% to 20% low vegetation coverage in 1989 to the unchanged area in 2021. This part of the area is mainly the lower reaches of the Hailar River and the area within the area. As far as Huhe Noer Lake, Chagannao Ri Lake, and other water areas are concerned, the change represented by B is the area with no change from 0% to 20% low vegetation coverage from 1989 to 2021. This part of the area is mainly the lower reaches of the Hai La Er River and the water area of Huhe Nuoer Lake and Chagannao Ri Lake in the region. The change represented by D is the area with no change from 40% to 60% medium-high vegetation coverage from 1989 to 2021. This part of the area is mainly Hulun Buir Sandy Land, with an area of 144.94 km^2. The change represented by E is the area with no change from 60% to 100% high vegetation coverage from 1989 to 2021. This part of the area is evenly distributed throughout the study area, and its area is 1747.69 km^2.

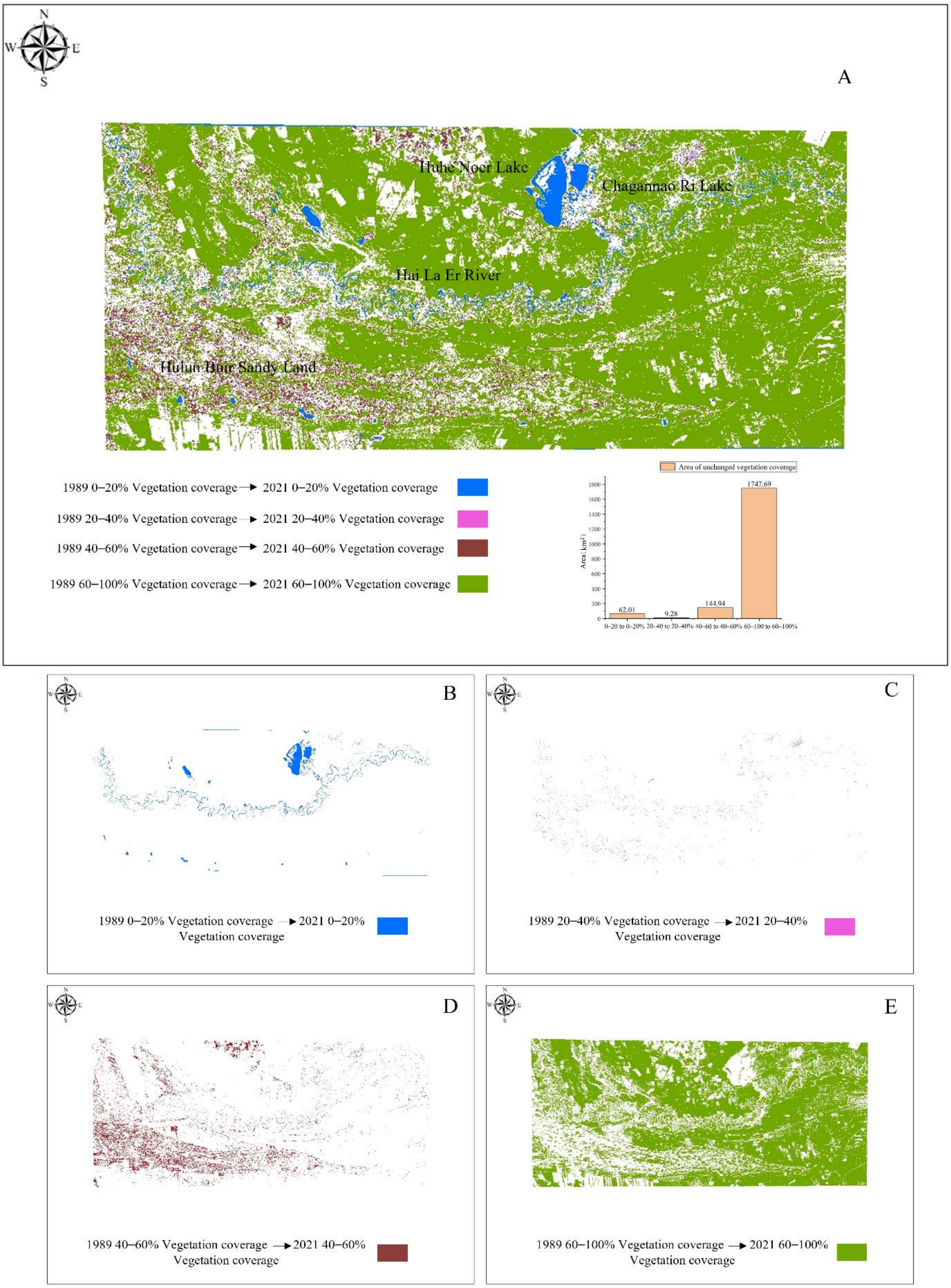

Figure 12. (**A**) Areas without any changes in vegetation cover in the 1989–2021 time scenario; (**B**): the area of 1989 0–20% vegetation coverage unchange to 2021 0–20% vegetation coverage; (**C**): the area of 1989 20–40% vegetation coverage unchange to 2021 20–40% vegetation coverage; (**D**): the area of 1989 40–60% vegetation coverage unchange to 2021 40–60% vegetation coverage; (**E**): the area of 1989 60–100% vegetation coverage unchange to 2021 60–100% vegetation coverage.

The Hulun Buir grassland research area is located in a temperate semi-arid climate zone, and the vegetation types are mainly grassland, shrubs, and xerophyte herbs [41]. After the 1990s, the local people's awareness of returning farmland to forests increased, and they began to gradually plant trees and grasses. Urban construction and rural land systems prohibited indiscriminate reclamation of land. The vegetation and environmental conditions were well adapted. At the same time, due to the continuous improvement of local policies and ecological awareness, the water area in the region increased, the vegetation growth environment improved, the expansion of the sandy land in Hulun Buir curbed, and the ecological environment in the region improved [9]. At the same time, it also provided a good living space for vegetation. Thereby, most of the Hulun Buir grassland with high vegetation coverage can remain unchanged. The changes in vegetation coverage reflected by the change in FVC are positive and optimistic in the study area.

5.3. Vegetation Change Process and Reasons

The vegetation changes are affected by various anthropogenic and natural factors, such as water supply, rainfall, and human activities [41,42]. According to the previously reported works in the literature, the vegetation shows a green trend due to climate change, the growth period is prolonged, and the photosynthesis intensity is increased [43,44]. The authors found that the increase in the vegetation cover in northern China before the 1990s was attributed to the warming and elevated precipitation, while the drought and rainfall reduction caused by climate warming after the 1990s led to the decline of vegetation cover. Peng et al., 2011 found that in arid and semi-arid grassland areas, precipitation is the main factor affecting vegetation growth [45].

The impact of climate on vegetation changes is as follows: The ecological environment of the study area in the hinterland of Hulun Buir grassland is relatively complex and diverse, including grassland, swamp wetlands, floodplain meadows, shrubs, and other ecosystems. Figure 13 depicts the annual average data of temperature and rainfall in the Hai La Er region from 1989 to 2020, compiled in this work. The overall temperature and rainfall showed a downward trend. In addition, rainfall has a great impact on vegetation coverage. For example, in 1999, the average annual rainfall in the study area was 276.4 mm, and the average annual temperature was −0.49 °C, which was significantly lower than the climatic element data of the adjacent 1998 and 2000 years. Therefore, the vegetation coverage in 1999 showed a large area of low rainfall and low temperatures. The areas were covered by low to moderate levels of vegetation cover. The study area is located in the alpine region of Northeast China. With the decrease in the annual temperature, the permafrost of the soil increased, and the cold storage of the permafrost constituted a cooling control system, which led to an increase in the soil water content. At the same time, the temperature decreased and the vegetation and soil evapotranspiration decreased. These reasons generally play a role in promoting vegetation growth [46]. The Hulun Buir Sandy Land is due to the deforestation of the Pinus sylvestris forest from Hulun Lake to the western suburbs of Hai La Er when the former Soviet Union aided the construction of the railway, resulting in the desertification of the land. Historically, affected by human activities, vegetation has been severely damaged, resulting in land degradation. There are certain difficulties in the reconstruction. However, according to our monitoring data, the overall coverage of the Hulun Buir Sandy Land has been significantly improved, reflecting that the ecological quality of the area has improved. Our research results are also consistent with those of [44]. Vegetation cover change is driven by climate change and human activities, which change the concentration of vegetation cover.

The influence of human activities on vegetation changes is as follows: Hulun Buir grassland is one of the key areas of ecological construction in my country. With the development of the local economy, the continuous increase in the regional GDP, the influence of population growth and industrial development, etc., it has become the main driving force for the expansion of land use in the Hai La Er region, affecting the vegetation growth environment and over-exploitation of water resources, making the contradiction between the regional development and the ecological environment increasingly increasing and having a profound impact on vegetation changes in the region. How to balance regional economic development and protection of the ecological environment deserves our deep consideration. In recent years, a series of vegetation protection projects have been released by China and local governments [9]. Through a series of human interventions, regional vegetation has been developed and protected. Therefore, in order to protect and restore wetlands ecologically, sustainable management of naturally vegetated areas is still required.

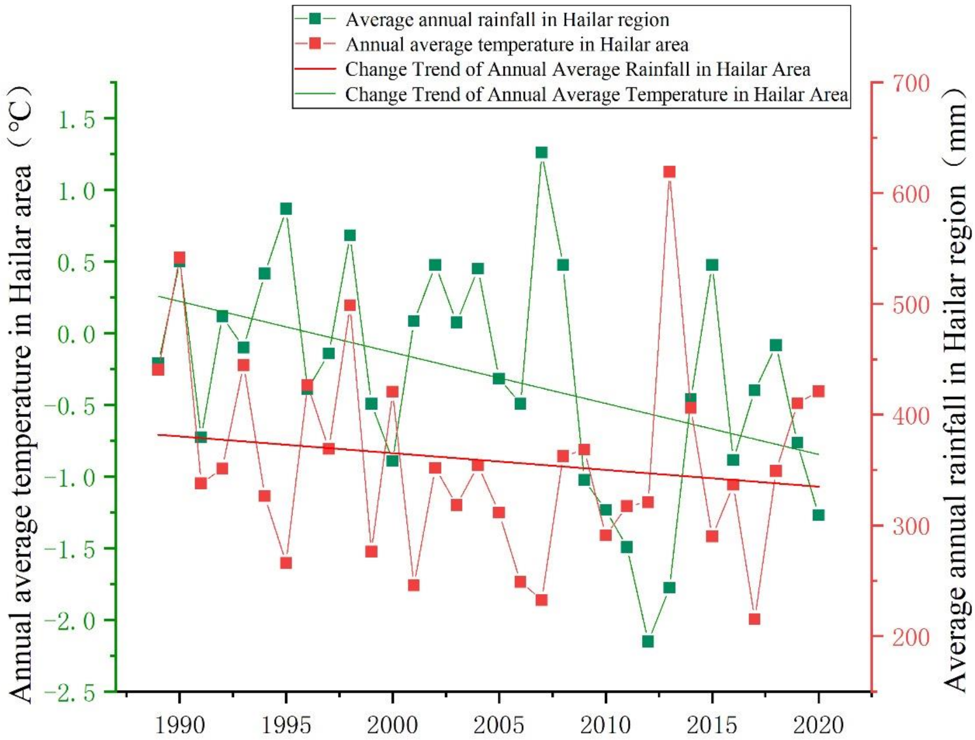

Figure 13. Trends in annual average temperature and annual rainfall in Hai La Er from 1989 to 2021.

5.4. Evaluation of Vegetation Cover Change Monitoring Model

In recent years, the vegetation cover change and its driving factors have been examined in the literature [7,8,27]. As an effective indicator to measure vegetation growth, vegetation coverage (FVC) is widely used to monitor the vegetation changes at regional and even global scales [19–21]. The results of vegetation coverage change reveal the spatial variation degree of the regional vegetation coverage. The spatial variation of regional vegetation coverage during the study period showed great temporal and spatial variation. This technology can easily provide a change matrix, from which the different transfers from one planting area to another can be intuitively detected. Thus, the change areas and the transformation of vegetation cover between different categories are clearly shown [9].

In this work, based on the Landsat data of the summer vegetation growth seasons in 1989, 1999, 2011, and 2021, the vegetation cover change scenarios in the study area at three time points in 1989, 1999, and 2011 were compared. It was proposed to develop a vegetation coverage change model and realize this spatial transformation monitoring model through Matlab programming, which was used to monitor the change of vegetation coverage at characteristic time nodes. This model started from the classification step of vegetation coverage of remote sensing images. Then, there is the transition monitoring step, which finally identifies the changed regions as pixel-to-pixel differences. Compared with previous vegetation cover models, the newly proposed model in this study was developed based on long-term time-series satellite digital change monitoring. Most previous studies on regional-scale vegetation change assessment have used remote sensing images of land cover and land use maps to analyze vegetation changes. In contrast, the vegetation cover change monitoring model proposed in this work performs well in monitoring and evaluating the regional scale vegetation cover change in a long time-series. This digital change-based vegetation cover monitoring and evaluation method has better monitoring accuracy and enforceability and is conducive to the regional scale vegetation diversity, ecosystem process, and other related research.

There are limitations of vegetation cover change models and environmental constraints. Our monitoring was greatly affected by the data quality, and the restricted environmental factors are obvious. Limiting environmental factors include atmospheric conditions (clouds and fog), which generally have a greater impact in summer or autumn. However, summer and autumn are the seasons with obvious vegetation changes, and the low time frequency and quality of these seasonal data affect our model monitoring results. The internal limiting factors of vegetation are as follows: We only pay attention to the change of the overall vegetation coverage classification interval. However, the internal succession of vegetation affects the monitoring results, and the evaluation of the effectiveness of these potential impacts will be addressed in further research.

6. Conclusions

Based on Landsat data and the Matlab platform, a new model for monitoring the spatial change of vegetation cover was proposed here, which was used to monitor the change of vegetation cover in the hinterland of Hulun Buir grassland in the past 30 years from 1989 to 2021. The results show that:

It was demonstrated that the vegetation cover model proposed in this work can be used to reveal and describe changes in large-scale vegetation landscapes, with easily accessible data and clear results in vegetation changes, with low technical cost, and can be used in most large-scale platform applications.

The data obtained by the vegetation coverage change monitoring model show that there are spatial differences in the vegetation coverage change area. The total area of vegetation coverage changes was 758.95 km^2, and the area from vegetation coverage above low to high vegetation coverage was 456.41 km^2, accounting for 60.14% of the total change area. The area changed from high vegetation coverage to low vegetation coverage was 302.57 km^2, accounting for 39.86% of the total change area. From 1989 to 2021, the vegetation coverage in the hinterland of the Hulunbuir grassland has generally improved.

Due to the local policy orientation and the continuous improvement of ecological awareness, the vegetation growth environment has been improved, the expansion of the sandy land in Hulun Buir has been curbed, and the ecological environment in the region has been enhanced. As a result, the research area in the hinterland of the Hulun Buir grassland has a large area without vegetation coverage. The area without vegetation coverage was 1963.92 km^2, accounting for 72.13% of the study area.

In the process of pursuing regional economic development and accelerating urbanization, industrialization, and agricultural modernization, human beings should develop in harmony with the natural environment. More responsibility to protect the ecological environment is required while pursuing the sustainable development of the natural environment.

Author Contributions: Conceptualization, X.D. and C.H.; methodology, X.D.; software, X.D.; validation, X.D. and C.H.; formal analysis, X.D.; investigation, X.D.; resources, X.D.; data curation, X.D.; writing—original draft preparation, X.D.; writing—review and editing, X.D.; visualization, X.D.; supervision, C.H.; project administration, C.H.; funding acquisition, C.H. All authors have read and agreed to the published version of the manuscript.

Funding: This work was funded by the National Natural Science Foundation of China (U2102209).

Institutional Review Board Statement: Not applicable.

Informed Consent Statement: Not applicable.

Data Availability Statement: Data are not available.

Acknowledgments: X.D. wishes to thank C.H. for his guidance on this paper.

Conflicts of Interest: The authors declare no conflict of interest.

References

1. Jonathan, A.; Foley, S.L.A.M.H.C.E.A. Incorporating Dynamic Vegetation Cover Within Global Climate Models. *Ecol. Appl.* **2010**, *10*.
2. Zhu, Z.; Xu, L.; Bi, J.; Myneni, R.; Knyazikhin, Y. Attribution of trends in global vegetation greenness from 1982 to 2011. *Am. Geophys. Union* **2012**, *2012*, GC23B-1058.
3. Zuo, Y.; Li, Y.; He, K.; Wen, Y. Temporal and spatial variation characteristics of vegetation coverage and quantitative analysis of its potential driving forces in the Qilian Mountains, China, 2000–2020. *Ecol. Indic.* **2022**, *143*, 109429. [CrossRef]
4. Huo, H.; Sun, C. Spatiotemporal variation and influencing factors of vegetation dynamics based on Geodetector: A case study of the northwestern Yunnan Plateau, China. *Ecol. Indic.* **2021**, *130*, 108005. [CrossRef]
5. Zhang, Y.; Ye, A. Quantitatively distinguishing the impact of climate change and human activities on vegetation in mainland China with the improved residual method. *GIScience Remote Sens.* **2021**, *58*, 235–260. [CrossRef]
6. Feng, D.; Fu, M.; Sun, Y.; Bao, W.; Zhang, M.; Zhang, Y.; Wu, J. How Large-Scale Anthropogenic Activities Influence Vegetation Cover Change in China? A Review. *Forests* **2021**, *12*, 320. [CrossRef]
7. Gu, Z.; Duan, X.; Shi, Y.; Li, Y.; Pan, X. Spatiotemporal variation in vegetation coverage and its response to climatic factors in the Red River Basin, China. *Ecol. Indic.* **2018**, *93*, 54–64. [CrossRef]
8. Guo, E.; Wang, Y.; Wang, C.; Sun, Z.; Bao, Y.; Mandula, N.; Li, H. NDVI Indicates Long-Term Dynamics of Vegetation and Its Driving Forces from Climatic and Anthropogenic Factors in Mongolian Plateau. *Remote Sens.* **2021**, *13*, 688. [CrossRef]
9. Dong, X.; Chen, Z. Digital Examination of Vegetation Changes in River Floodplain Wetlands Based on Remote Sensing Images: A Case Study Based on the Downstream Section of Hailar River. *Forests* **2021**, *12*, 1206. [CrossRef]
10. Dong, X.; Chen, Z.; Wu, M.; Hu, C. Long time series of remote sensing to monitor the transformation research of Kubuqi Desert in China. *Earth Sci. Inform.* **2020**, *13*, 795–809. [CrossRef]
11. Lin, M.; Hou, L.; Qi, Z.; Wan, L. Impacts of climate change and human activities on vegetation NDVI in China's Mu Us Sandy Land during 2000–2019. *Ecol. Indic.* **2022**, *142*, 109164. [CrossRef]
12. Shi, P.; Li, P.; Li, Z.; Sun, J.; Wang, D.; Min, Z. Effects of grass vegetation coverage and position on runoff and sediment yields on the slope of Loess Plateau, China. *Agric. Water Manag.* **2022**, *259*, 107231. [CrossRef]
13. Sang, S.; Song, S.; Li, F.; Yu, M.; Yu, G.; Zhang, Q.; Wu, Y. Vegetation coverage changes driven by a combination of climate change and human activities in Ethiopia, 2003–2018. *Ecol. Inform.* **2022**, *71*, 101776.
14. Zhang, C.; Kuai, S.; Tang, C.; Zhang, S. Evaluation of hydrological connectivity in a river floodplain system and its influence on the vegetation coverage. *Ecol. Indic.* **2022**, *144*, 109445. [CrossRef]
15. Zhang, X.; Song, J.; Wang, Y.; Sun, H.; Li, Q. Threshold effects of vegetation coverage on runoff and soil loss in the Loess Plateau of China: A meta-analysis. *Geoderma* **2022**, *412*, 115720. [CrossRef]
16. Pan, N.; Feng, X.; Fu, B.; Wang, S.; Ji, F.; Pan, S. Increasing global vegetation browning hidden in overall vegetation greening: Insights from time-varying trends. *Remote Sens. Environ.* **2018**, *214*, 59–72. [CrossRef]
17. Li, Z.; Zhang, Y.; Zhu, Q.; He, Y.; Yao, W. Assessment of bank gully development and vegetation coverage on the Chinese Loess Plateau. *Geomorphology* **2015**, *228*, 462–469. [CrossRef]
18. Yao, J.; Cheng, J.; Zhou, Z.; Sun, L.; Zhang, H. Effects of herbaceous vegetation coverage and rainfall intensity on splash characteristics in northern China. *Catena* **2018**, *167*, 411–421. [CrossRef]
19. Zhang, X.; Pei, Q.; Chen, Y.; Guo, Y.; Hou, Y.; Sun, R. Study on Temporal and Spatial Change of Vegetation Coverage in Haiyan County Based on GF-1. *Procedia Comput. Sci.* **2019**, *162*, 642–650. [CrossRef]
20. Zhang, P.; Cai, Y.; Yang, W.; Yi, Y.; Yang, Z.; Fu, Q. Multiple spatio-temporal patterns of vegetation coverage and its relationship with climatic factors in a large dam-reservoir-river system. *Ecol. Eng.* **2019**, *138*, 188–199. [CrossRef]
21. Rezaei, A.; Gurdak, J.J. Large-scale climate variability controls on climate, vegetation coverage, lake and groundwater storage in the Lake Urmia watershed using SSA and wavelet analysis. *Sci. Total Environ.* **2020**, *724*, 138273. [CrossRef] [PubMed]
22. Han, W.; Zhao, S.; Feng, X.; Chen, L. Extraction of multilayer vegetation coverage using airborne LiDAR discrete points with intensity information in urban areas: A case study in Nanjing City, China. *Int. J. Appl. Earth Obs. Geoinf.* **2014**, *30*, 56–64. [CrossRef]
23. Duo, A.; Zhao, W.; Qu, X.; Jing, R.; Xiong, K. Spatio-temporal variation of vegetation coverage and its response to climate change in North China plain in the last 33 years. *Int. J. Appl. Earth Obs. Geoinf.* **2016**, *53*, 103–117.
24. Zhang, C.; Lu, D.; Chen, X.; Zhang, Y.; Maisupova, B.; Tao, Y. The spatiotemporal patterns of vegetation coverage and biomass of the temperate deserts in Central Asia and their relationships with climate controls. *Remote Sens. Environ.* **2016**, *175*, 271–281. [CrossRef]
25. Duan, C.; Wu, L.; He, L.; Wang, S. Spatio-temporal distribution pattern of vegetation coverage in Junggar Basin, Xinjiang. *Acta Ecol. Sin.* **2016**, *36*, 72–76. [CrossRef]
26. Guo, Z.C.; Wang, T.; Liu, S.L.; Kang, W.P.; Chen, X.; Feng, K.; Zhi, Y. Biomass and vegetation coverage survey in the Mu Us sandy land-based on unmanned aerial vehicle RGB images. *Int. J. Appl. Earth Obs. Geoinf.* **2021**, *94*, 102239. [CrossRef]

27. Li, D.; Lu, D.; Zhao, Y.; Zhou, M.; Chen, G. Spatial patterns of vegetation coverage change in giant panda habitat based on MODIS time-series observations and Local Indicators of Spatial Association. *Ecol. Indic.* **2021**, *124*, 107418. [CrossRef]
28. Jou, R.M.; Macario, K.D.; Pessenda, L.C.; Pereira, M.G.; Lorente, F.L.; Pedrosa, R.; Cardoso, R.P. The use of carbon isotopes (13C, 14C) in different soil types and vegetation coverage in a montane atlantic forest region, Southeast Brazil. *Quat. Geochronol.* **2021**, *61*, 101133. [CrossRef]
29. Zhu, L.; Ke, Y.; Hong, J.; Zhang, Y.; Pan, Y. Assessing degradation of lake wetlands in Bashang Plateau, China based on long-term time series Landsat images using wetland degradation index. *Ecol. Indic.* **2022**, *139*, 108903. [CrossRef]
30. Hao, J.; Chen, X.; Zhang, Z.; Gao, Y.; Li, L.; Li, H. Quantifying the temporal-spatial scale dependence of the driving mechanisms underlying vegetation coverage in coastal wetlands. *Catena* **2021**, *204*, 105435. [CrossRef]
31. Fang, Q.; Wang, G.; Zhang, S.; Peng, Y.; Xue, B.; Cao, Y.; Shrestha, S. A novel ecohydrological model by capturing variations in climate change and vegetation coverage in a semi-arid region of China. *Environ. Res.* **2022**, *211*, 113085. [CrossRef] [PubMed]
32. Li, J.; Wang, J.; Zhang, J.; Liu, C.; He, S.; Liu, L. Growing-season vegetation coverage patterns and driving factors in the China-Myanmar Economic Corridor based on Google Earth Engine and geographic detector. *Ecol. Indic.* **2022**, *136*, 108620. [CrossRef]
33. Dong, X.; Hu, C. A new method for describing the inundation status of floodplain wetland. *Ecol. Indic.* **2021**, *131*, 108144. [CrossRef]
34. Li, S.; Wang, J.; Zhang, M.; Tang, Q. Characterizing and attributing the vegetation coverage changes in North Shanxi coal base of China from 1987 to 2020. *Resour. Policy* **2021**, *74*, 102331. [CrossRef]
35. Li, J.; Wang, J.; Zhang, J.; Zhang, J.; Kong, H. Dynamic changes of vegetation coverage in China-Myanmar economic corridor over the past 20 years. *Int. J. Appl. Earth Obs. Geoinf.* **2021**, *102*, 102378. [CrossRef]
36. Song, W.; Mu, X.; Ruan, G.; Gao, Z.; Li, L.; Yan, G. Estimating fractional vegetation cover and the vegetation index of bare soil and highly dense vegetation with a physically based method. *Int. J. Appl. Earth Obs. Geoinf.* **2017**, *58*, 168–176. [CrossRef]
37. Zhao, A.; Zhang, A.; Lu, C.; Wang, D.; Wang, H.; Liu, H. Spatiotemporal variation of vegetation coverage before and after implementation of Grain for Green Program in Loess Plateau, China. *Ecol. Eng.* **2017**, *104*, 13–22. [CrossRef]
38. Yao, X.; Wu, J.; Gong, X.; Lang, X.; Wang, C.; Song, S.; Ahmad, A. A Effects of long term fencing on biomass, coverage, density, biodiversity and nutritional values of vegetation community in an alpine meadow of the Qinghai-Tibet Plateau. *Ecol. Eng.* **2019**, *130*, 80–93. [CrossRef]
39. De Jong, R.; de Bruin, S.; de Wit, A.; Schaepman, M.E.; Dent, D.L. Analysis of monotonic greening and browning trends from global NDVI time-series. *Remote Sens. Environ.* **2011**, *115*, 692–702. [CrossRef]
40. Wang, X.; Peng, S.; Ling, H.; Xu, H.; Ma, T. Do Ecosystem Service Value Increase and Environmental Quality Improve due to Large–Scale Ecological Water Conveyance in an Arid Region of China? *Sustainability* **2019**, *11*, 6586. [CrossRef]
41. Li, D.; Zhang, C.; Pizzol, L.; Critto, A.; Zhang, H.; Lv, S.; Marcomini, A. Regional risk assessment approaches to land planning for industrial polluted areas in China: The Hulunbeier region case study. *Environ. Int.* **2014**, *65*, 16–32. [CrossRef] [PubMed]
42. Shi, S.; Yu, J.; Wang, F.; Wang, P.; Zhang, Y.; Jin, K. Quantitative contributions of climate change and human activities to vegetation changes over multiple time scales on the Loess Plateau. *Sci. Total Environ.* **2021**, *755*, 142419. [CrossRef] [PubMed]
43. Dragoni, D.; Schmid, H.P.; Wayson, C.A.; Potter, H.; Grimmond, C.S.B.; Randolph, J.C. Evidence of increased net ecosystem productivity associated with a longer vegetated season in a deciduous forest in south-central Indiana, USA. *Glob. Chang. Biol.* **2011**, *17*, 886–897. [CrossRef]
44. Gu, Y.; Pang, B.; Qiao, X.; Xu, D.; Li, W.; Yan, Y.; Zou, C. Vegetation dynamics in response to climate change and human activities in the Hulun Lake basin from 1981 to 2019. *Ecol. Indic.* **2022**, *136*, 108700. [CrossRef]
45. Peng, S.; Chen, A.; Xu, L.; Cao, C.; Fang, J.; Myneni, R.B.; Piao, S. Recent change of vegetation growth trend in China. *Environ. Res. Lett.* **2011**, *6*, 044027. [CrossRef]
46. Dong, X.; Hu, C.; Liu, P. Study on the Coupling Relationship among Climate, Runoff and Floodplain Wetland Inundation–Taking the Lower Reach of Hailar River as an Example. *J. Ecol.* **2022**, *42*.